

1 **RECONSTRUCTING HUMAN MOBILITY PATTERN: A SEMI-SUPERVISED**
2 **APPROACH FOR CROSS-DATASET TRANSFER LEARNING**

3

4

5

6 **Xishun Liao, Ph.D.**

7 Civil and Environmental Engineering Department

8 University of California, Los Angeles, Los Angeles, California, 90095

9 xishunliao@ucla.edu

10

11 **Yifan Liu**

12 Civil and Environmental Engineering Department

13 University of California, Los Angeles, Los Angeles, California, 90095

14 bmmliu@ucla.edu

15

16 **Chenchen Kuai**

17 Civil and Environmental Engineering Department

18 Texas A&M University, College Station, Texas, 77840

19 mobility@tamu.edu

20

21 **Yueshuai He, Ph.D.**

22 Civil and Environmental Engineering Department

23 University of Louisville, Louisville, Kentucky, 40208

24 yueshuai.he@louisville.edu

25

26 **Shangqing Cao**

27 Department of Civil and Environmental Engineering

28 University of California, Berkeley, Berkeley, California 94720

29 caoalbert@berkeley.edu

30

31 **Chris Stanford, Ph.D.**

32 Novateur Research Solutions

33 20110 Ashbrook Place, STE 170, Ashburn, VA 20147

34 cstanford@novateur.ai

35

36 **Jiaqi Ma, Ph.D., Corresponding Author**

37 Civil and Environmental Engineering Department

38 University of California, Los Angeles, Los Angeles, California, 90095

39 jiaqima@ucla.edu

40

41

42 Word Count: 6733 words + 3 table(s) × 250 = 7483 words

43

44

45

1

2

3

4 Submission Date: August 1, 2024

1 ABSTRACT

2 Understanding human mobility patterns is crucial for urban planning, transportation management,
3 and public health. This study tackles two primary challenges in the field: the reliance on trajectory
4 data, which often fails to capture the semantic interdependencies of activities, and the inherent
5 incompleteness of real-world trajectory data. We have developed a model that reconstructs and
6 learns human mobility patterns by focusing on semantic activity chains. We introduce a semi-
7 supervised iterative transfer learning algorithm to adapt models to diverse geographical contexts
8 and address data scarcity. Our model is validated using comprehensive datasets from the United
9 States, where it effectively reconstructs activity chains and generates high-quality synthetic mobility
10 data, achieving a low Jensen-Shannon Divergence (JSD) value of 0.001, indicating a close similarity
11 between synthetic and real data. Additionally, sparse GPS data from Egypt is used to evaluate
12 the transfer learning algorithm, demonstrating successful adaptation of US mobility patterns to
13 Egyptian contexts, achieving a 64% of increase in similarity, i.e., a JSD reduction from 0.09 to 0.03.
14 This mobility reconstruction model and the associated transfer learning algorithm show significant
15 potential for global human mobility modeling studies, enabling policymakers and researchers to
16 design more effective and culturally tailored transportation solutions.

17

18 *Keywords:* Human Mobility Patterns Modeling, Transfer Learning, Semi-Supervised Learning,
19 Synthetic Mobility Data

1 INTRODUCTION

2 Understanding human mobility patterns has become increasingly crucial in various fields, including
3 urban planning, transportation management (1, 2), and public health (3). As urbanization accelerates
4 and population mobility increases, the ability to accurately comprehend and predict human activity
5 patterns has gained paramount importance. This knowledge not only aids in optimizing urban
6 resource allocation but also provides essential insights for the development of smart cities.

7 However, current research on human mobility patterns faces two significant challenges.
8 First, most studies rely heavily on trajectory data to analyze spatio-temporal patterns, which often
9 fall short in capturing the underlying semantic interdependency among activities. This approach
10 fails to answer critical questions about human behavior, such as how people schedule their daily
11 activities, what activities typically follow one another, and how activities are distributed within a
12 day (e.g., working and school period). Understanding these semantic relationships is crucial for
13 developing a comprehensive model of human mobility.

14 The second challenge stems from the nature of real-world trajectory data, typically collected
15 through GPS-enabled devices like smartphones (4–7). Due to the intermittent nature of data
16 collection and privacy concerns, these datasets often provide incomplete or fragmented views of
17 individuals' daily mobility pattern. This incompleteness makes it difficult to model and understand
18 the full spectrum of human activities and their interdependencies throughout a day or across different
19 contexts.

20 To address these challenges, innovative approaches that can understand and then reconstruct
21 semantic activity chains are in demand. Such methods must be capable of inferring missing activities,
22 understanding activity dependencies, and capturing the temporal patterns of human behavior. Recent
23 studies have explored annotating human trajectories with semantic information, linking activities
24 to trajectories, which enables the use of natural language processing (NLP) techniques on these
25 annotated trajectories (8, 9). Even though with more semantic information, developing these
26 models to learn mobility pattern is still particularly complex when dealing with incomplete datasets,
27 especially in regions where comprehensive ground truth data is unavailable, rendering traditional
28 supervised learning approaches ineffective. In such scenarios, we must explore alternative methods
29 that can leverage incomplete datasets, leading us to consider semi-supervised learning techniques
30 and transfer learning approaches.

31 In this paper, we propose a model for reconstructing and learning human mobility patterns,
32 focusing specifically on semantic activity chains. This model captures common patterns across
33 agents, learns activity dependencies, and understands the characteristics of each activity, allowing
34 to effectively reconstruct and infer missing parts of activity chains. Furthermore, considering that
35 human mobility patterns vary across different regions due to cultural and environmental factors, and
36 recognizing the challenge of modeling these patterns in areas with limited or fragmented activity
37 data, we propose a novel semi-supervised approach for cross-dataset transfer learning. This learning
38 strategy addresses the limitations of traditional supervised learning, which requires ground truth
39 data, and enables effective cross-dataset and cross-region knowledge transfer. Consequently, this
40 semi-supervised transfer learning approach allows our model to adapt to diverse geographical
41 contexts and overcome data scarcity issues.

42 With such capability for human mobility reconstruction and knowledge transfer, this model
43 offers significant potential for urban planning, policy development, and transportation system
44 analysis across diverse regions. It serves as a powerful tool for data augmentation, enabling the
45 generation of high-quality synthetic mobility data in areas with limited observational data. This

1 approach facilitates comprehensive data mining and analysis, providing insights into complex
2 mobility patterns. Furthermore, the model's ability to synthesize realistic mobility data significantly
3 advances the field of transportation modeling by enabling the automatic generation of sophisticated
4 simulation models.

5 Compared to existing literature, our research makes several significant contributions to the
6 field of human mobility pattern analysis:

- 7 • We propose a generic framework for modeling human mobility patterns across various
8 datasets, regions, and cultures. This framework demonstrates the effectiveness of cross-
9 dataset transfer learning, making it suitable for studying human mobility in data-scarce
10 environments.
- 11 • We introduce a novel approach to human activity pattern reconstruction, addressing the
12 limitations of current trajectory-based methods.
- 13 • Our semi-supervised iterative training method enables transfer learning for scenarios
14 lacking ground truth datasets, significantly expanding the applicability of mobility pattern
15 analysis.

16 RELATED WORKS

17 Human Travel Trajectory Reconstruction

18 Trajectory reconstruction has become crucial in understanding human mobility patterns, espe-
19 cially when dealing with incomplete datasets. Recent advancements have addressed challenges
20 of data sparsity and irregularity through innovative techniques. Chen et al. (10) introduced the
21 Context-enhanced Trajectory Reconstruction (CTR) method, using tensor factorization to recon-
22 struct complete individual trajectories from sparse Call Detail Records. Li et al. (11) proposed
23 the Multi-criteria Data Partitioning Trajectory Reconstruction (MDP-TR) method for large-scale,
24 low-frequency mobile phone datasets, enhancing reconstruction performance by considering spa-
25 tiotemporal patterns of missing data and individual similarities. For GPS data, Zheng et al. (12)
26 developed a collaborative system for location and activity recommendations, demonstrating signifi-
27 cant improvements in inferring activity types. Alexander et al. (13) emphasized the importance of
28 comprehensive temporal and spatial analysis in trajectory reconstruction using mobile phone data.

29 Despite these advancements, challenges persist, including the diverse characteristics of data
30 sources, limited data accessibility, and restricted model adaptability across different geographic
31 regions. These challenges underscore the need for continued research to develop more robust and
32 widely applicable reconstruction techniques.

33 Transfer Learning

34 Recent advancements in transfer learning have shown significant potential for enhancing human mo-
35 bility pattern analysis, particularly in scenarios with limited data. Techniques originally developed
36 for natural language processing offer valuable insights for trajectory reconstruction and mobility
37 modeling.

38 Howard and Ruder's (14) gradual unfreezing technique could be adapted to preserve general
39 mobility patterns while adjusting to specific regional characteristics. Peters et al. (15) and Merchant
40 et al. (16) suggest that middle layers are often the most transferable, which could be useful when
41 adapting mobility models from data-rich to data-scarce regions. Liu et al. (17) explored freezing
42 bottom layers while fine-tuning top layers, a strategy that could preserve fundamental human
43 movement patterns while adapting to unique characteristics of specific urban environments.

These studies collectively suggest strategies for enhancing trajectory reconstruction and mobility modeling through gradual adaptation of pre-trained models and selective fine-tuning of relevant layers. Future research should focus on adapting these methods to the unique characteristics of mobility data, considering spatiotemporal dependencies and the complex nature of human movement patterns. Such advancements could significantly improve our ability to model and predict human mobility, especially in regions with limited observational data.

PROBLEM STATEMENT

Reconstruction Task

We denote i for an agent. The j -the trajectory collected for the agent contains N stay points, $Traj_j^i = \{P_1^{i,j}, P_2^{i,j}, \dots, P_N^{i,j}\}$. Trajectories are annotated by one of our previous study (8), where each stay point is linked with an activity, where each stay point $P_n^{i,j} = [T_n^{i,j}, (x,y)^{i,j}, S_n^{i,j}, E_n^{i,j}]$ consists of activity type $T_n^{i,j}$ (as shown in Table 1), GPS location $(x,y)^{i,j}$, start time $S_n^{i,j}$ and end time $E_n^{i,j}$. Our goal is to develop a model that can capture the common activity patterns of a region. Therefore, we focus on modeling these activity patterns rather than learning the locations of the agent. An activity chain is a time-ordered sequence of activities, defined based on the annotated trajectory, $A_j^i = \{A_1^{i,j}, A_2^{i,j}, \dots, A_N^{i,j}\}$, where $A_n^{i,j} = [T_n^{i,j}, S_n^{i,j}, E_n^{i,j}]$.

Due to the fragmented nature of GPS-based data collection methods, stay points usually represent only certain moments of the day rather than covering the entire daily activity of the agent. As a result, the activity chain A_j in a real-world dataset is usually incomplete. For example, an observe recorded activities chain (in blue) is shown in the Figure 1. This chain includes "Home" from "02-01 00:00 to 02-01 07:00", "Work" from "02-01 08:00 to 02-01 10:00", "Home" from "02-02 00:00 to 02-02 04:00", and "Work" from "02-02 06:00 to 02-02 08:00". There are significant gaps in the recorded activities, particularly from "02-01 10:00 to 02-02 00:00" and from "02-02 08:00" onwards.

Finally, provided an incomplete activity chain in region $R1$, a model M^{R1} for region $R1$ can reconstruct possible missing daily activities, as shown by the dashed gray lines in the Figure 1, filling up the missing time slots based on the common activity pattern of the region. Based on the common activity pattern learned in this region, the model completes the "Work" periods, introduces "EatOut (buy meals)" activities, and proposes "Home" activities to complete the daily cycle, ensuring a reasonable activity chain.

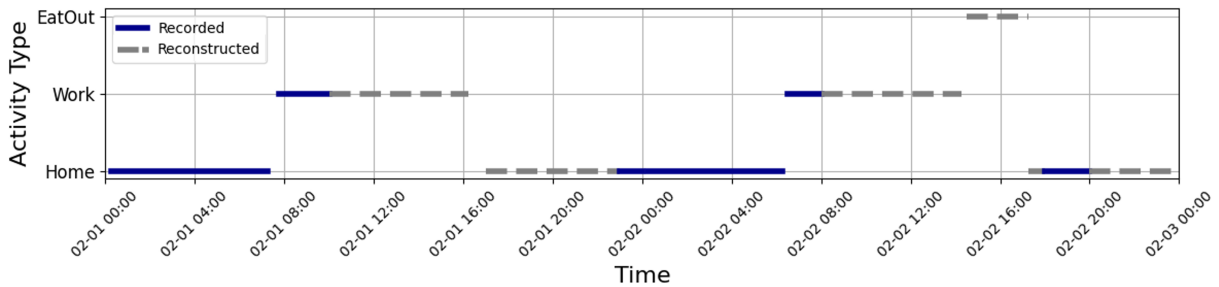


FIGURE 1: Reconstructed activity chain from an incomplete chain

1 **Performance Evaluation at System Level**

2 Given the inherent uncertainty in human behavior, predicting the original activity chain of a specific
 3 agent can be challenging and may not always be appropriate. Therefore, our model aims to common
 4 pattern, reasonable, align with the distribution of the target region. This approach allows for the
 5 reconstruction of plausible full-day activity chains while acknowledging the variability in individual
 6 behaviors.

7 The performance of the model is quantified at the system level by assessing the similarity
 8 between the distributions of generated and real-world (ground truth) activity patterns. In this paper,
 9 the Jensen-Shannon Divergence (JSD) is adopted as the similarity metric (18), as presented in
 10 Equation 1. The modeling objective is to minimize the difference between the distributions of the
 11 generated and ground truth activity patterns derived from activity chains. These metrics are 1)
 12 **activity frequencies**, 2) **start time**, 3) **end times**, 4) **number of daily activities** (i.e., length of
 13 activity chain), and 5) **duration of each activity**.

$$14 \quad JSD(P\|Q) = \frac{1}{2} \sum_{x \in X} \left[P(x) \log \left(\frac{P(x)}{M(x)} \right) \right] + \frac{1}{2} \sum_{x \in X} \left[Q(x) \log \left(\frac{Q(x)}{M(x)} \right) \right] \quad (1)$$

15 where $M = (P + Q)/2$. Here P represents the distribution of activity patterns extracted from the
 16 generated activity chains, while Q represents the distribution of activity patterns computed from
 17 ground truth activity chains. X represents the full range of probabilities with respect to a specific
 18 activity pattern statistic. As the JSD approaches zero, it indicates a higher level of similarity between
 19 the probability distributions being compared, thereby demonstrating the superior performance of
 20 model in approximating the true distribution.

21 **DATASET AND DATA CURATION**

22 **Dataset with Complete Activity Chain**

23 The training of the mobility pattern reconstruction model requires the use of complete activity chain,
 24 including every activity of an agent in a 24-hour day. Two datasets with completed activity chains
 25 were utilized in this study to construct the base model.

26 In order to learn common mobility patterns at the national level, we used the 2017 National
 27 Household Travel Survey (NHTS), administered by the Federal Highway Administration (FHWA),
 28 to capture nationwide mobility patterns (19). The NHTS includes socio-economic demographics
 29 and travel diaries from 129,600 households. We aggregated the original 19 activity types recorded
 30 in the NHTS into 15 categories based on the activity locations, which are presented in Table 1. In
 31 this study, only the travel diary of each agent in NHTS is used for training.

32 To learn a specific regional activity pattern, we adopted the activity chain data generated by
 33 the Activity-Based Model (ABM) of Southern California Association of Governments (SCAG). The
 34 SCAG ABM is a comprehensive modeling system that integrates a series of activity-related choice
 35 models, ranging from long-term to short-term decisions, to simulate the activity chains of residents
 36 in Southern California. This model generates a synthetic dataset that includes detailed information
 37 about the types and sequences of activities, locations, and start/end times. These features make
 38 the dataset a valuable tool for analyzing the spatiotemporal dynamics of human activities. Further
 39 details of the SCAG ABM and its methodology can be found in (20, 21).

TABLE 1: Activity category code and their corresponding descriptions

| | | | | | |
|----|--|----|--|----|---|
| 1 | Home activities (sleep, chores, etc) or Work from home | 2 | Work-related activity or Volunteer | 3 | Attend school |
| 4 | Attend child or adult care | 5 | Buy goods (groceries, clothes, gas) | 6 | Buy services (dry cleaners, banking, service a car) |
| 7 | Buy meals (go out for a meal, food, carry-out) | 8 | General errands (post office, library) | 9 | Recreational activities (visit parks, movies, bars) |
| 10 | Exercise (jog/walk, walk the dog, gym, etc) | 11 | Visit friends or relatives | 12 | Health care visit (medical, dental, therapy) |
| 13 | Religious or community activities | 14 | Something else | 15 | Drop off/pick up someone |

1 Real-World Trajectory Dataset Processing

2 Raw Data to Trajectory

3 In this study, we utilized GPS data collected in Egypt, provided by Veraset (22). This data, sourced
4 from devices such as smartphones and tablets equipped with location-based applications, exhibits
5 inherent randomness due to factors such as GPS drift and measurement error. To address this, we
6 developed a methodology to identify stay points to form the trajectory data of each agent.

7 Each record in the raw data is a tuple containing the user identification number, time stamp,
8 longitude, and latitude. We adopt a 2-step process to extract stay points from the raw data. Because a
9 record can be indicative of either a stay or movement, we first label records that are either 5 minutes
10 apart in time or 300 meters away in distance from the previous record as stays. Additionally, we
11 calculate the speed of the movement from the difference in both space and time between consecutive
12 records. Records that show a speed less than 30 kilometer per hour are kept as stay points.

13 The second step is to cluster all remaining records, which are now labeled as stay points,
14 into stay regions. The aggregation combines nearby stay points that are presumably a user's visits
15 to the same location. We adopt the clustering method outlined in (23), in which the entire region
16 covered by the dataset is divided into cells in a grid system, and the cells in the grid are assigned to
17 various stay regions according to the stay points detected. For this study, the resolution of the stay
18 regions we use is between 0.06378 km^2 and 0.12709 km^2 (level 9 hexagons in H3).

19 Activity Chain Construction by Trajectory Annotation

20 Based on the Point-of-interest (POI) data provided by Open Street Map (24) and GPS trajectories
21 identified as stay points, we create the activity chain by annotating each stay point with a corre-
22 sponding POI and activity. The process begins by using an LLM to match POIs with probable
23 activities; for example, a restaurant might be associated with activities like 'buy meal' and 'work'.
24 These categorized POIs with activities are then matched to each GPS-identified stay point, taking
25 into account the characteristics of POIs within a 25-meter radius and activities (8).

26 This whole activity chain construction process comprises two steps: first, the inference of
27 mandatory activities such as Home, Work, and School; and second, the inference of non-mandatory
28 activities. Since mandatory activities typically exhibit relatively consistent locations and periodic
29 patterns, we employ a rule-based method to infer them, as outlined in Alexander (25). For instance,
30 the 'Home' activity is identified by selecting the stay point that has the highest visit frequency during
31 night hours across up to six months. On the other hand, we employ a Bayesian-based algorithm to
32 identify non-mandatory activities at each stay point.

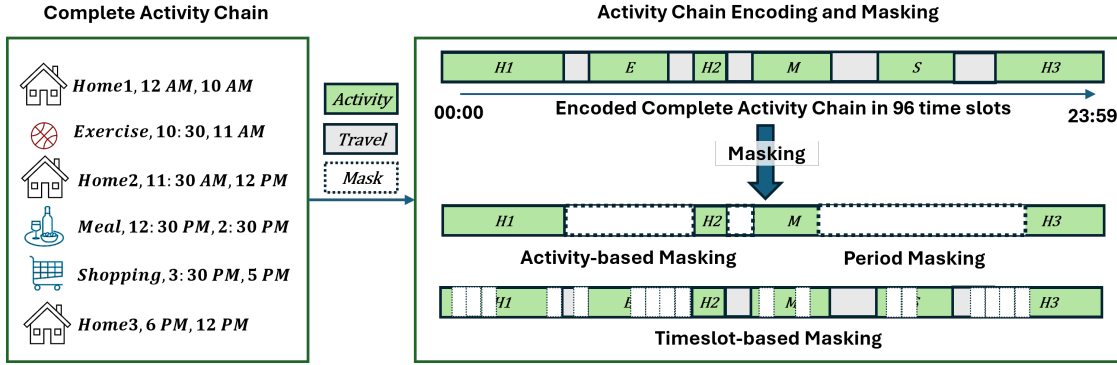


FIGURE 2: Activity encoding and masking approaches

1 This algorithm (8) evaluates the probability of each non-mandatory activity type T_i linked
 2 to POIs at a stay point, by considering factors such as the activity start time S and the characteristics
 3 associated with involved POIs . To construct the activity chain, we assign each stay point with the
 4 activity with highest probability, as the equation below:

$$5 \quad T = \arg \max_{T_i} \{P(T_i | \text{POI}, S)\} = \arg \max_{T_i} \left\{ \sum_j P(T_i | \text{POI}_j, S) \cdot P(\text{POI}_j) \right\} \quad (2)$$

6 where T is the activity at the stay point, given J POIs and start time S .

7 Activity Chain Encoding and Masking

8 To effectively process and learn from activity chains, we implement an encoding and masking
 9 strategy that allows our model to handle diverse activity sequences and simulate incomplete data
 10 scenarios. We encode a day's activity chain into a sequence of 96 time slots, each representing a
 11 15-minute interval. This fine-grained representation allows us to capture detailed temporal patterns
 12 of activities. Each activity in the chain is assigned to its corresponding time slots based on its start
 13 and end times. For instance, in the Figure 2 shown, "Home1" occupies the slots from 00:00 to 10:00,
 14 followed by a 30 minute travel time, then "Exercise" from 10:30 to 11:00, and so forth.

15 To train our model to reconstruct missing parts of activity sequences and enhance its
 16 robustness to incomplete data, we employ three distinct masking strategies that simulate common
 17 data missing scenarios encountered in real-world datasets. The first strategy, **activity-based**
 18 **masking**, involves randomly masking entire activities within the chain, simulating scenarios
 19 where specific activities are entirely missing from the data. The strategy, **period masking**, masks
 20 continuous periods of the day, irrespective of activity boundaries, mimicking situations where data
 21 for extended periods is unavailable. The third approach is **time slot-based masking**, which randomly
 22 masks individual time slots throughout the day, representing sporadic data loss or intermittent data
 23 collection.

24 These masking strategies simulate incomplete real-world data, enrich training examples, and
 25 push the model to robustly represent activity patterns and their interdependencies. By encoding and
 26 masking complete activity chain datasets, we generate a diverse corpus that enhances the model's
 27 ability to reconstruct activities comprehensively. This method is important for handling incomplete
 28 data and transferring knowledge to data-sparse regions. Additionally, applying various masking
 29 techniques to the same activity chain substantially increases the training data volume, improving

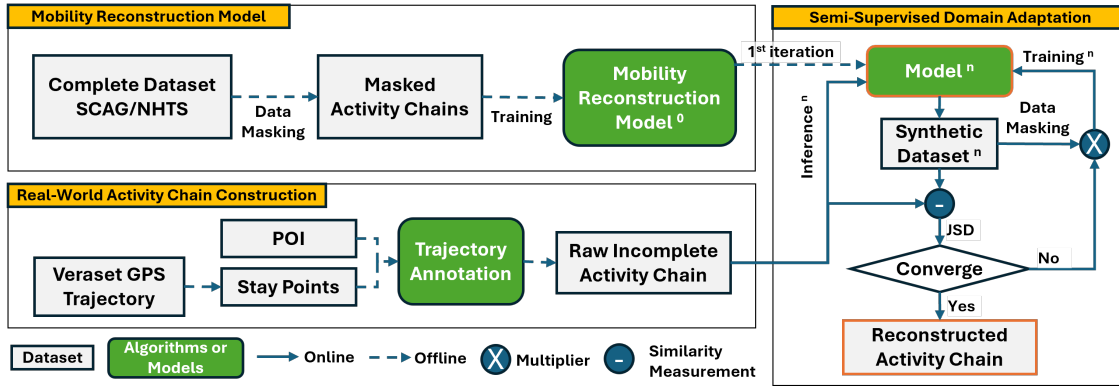


FIGURE 3: System Workflow for building transferable mobility reconstruction models

1 the model's predictive performance and generalizability across different patterns and contexts.

2 METHODOLOGY

3 System Workflow

4 The workflow of the proposed mobility reconstruction system is structured to optimally leverage
 5 comprehensive household travel survey data for application in less data-rich environments, as
 6 illustrated in Figure 3. It integrates the principles of semi-supervised domain adaptation in a novel
 7 methodological framework that does not rely on ground truth data.

8 The process initiates with the **training of the Mobility Reconstruction Model M^0** using
 9 a comprehensive dataset (e.g., NHTS and SCAG dataset) from data-rich regions like the United
 10 States, incorporating detailed activity chains from household travel surveys. This model undergoes
 11 training with various masking techniques that mimic scenarios of data incompleteness, enhancing
 12 its ability to handle real-world data variations effectively. After training, **real-world activity chains**
 13 **construction** occurs through data mining techniques applied to GPS trajectory data, focusing
 14 on extracting stay points and annotating trajectories with contextual data from points of interest
 15 (POIs). These chains remain inherently incomplete, mirroring typical data gaps in datasets. The
 16 **semi-supervised domain adaptation** module then starts, introducing a fine-tuning strategy to adapt
 17 the base mobility reconstruction model to regions with limited and incomplete data, bypassing the
 18 need for ground truth data.

19 This process, which begins by leveraging a complete dataset from a data-rich region and
 20 then transferring this knowledge to regions with limited or fragmented activity data, embodies an
 21 innovative iterative process of data synthesis and model refinement. It not only facilitates the robust
 22 prediction of activity patterns in regions lacking comprehensive data but also enhances the model's
 23 generalizability across various geographical contexts.

24 Model Design

25 Model Structure

26 The core of our approach is a sophisticated model architecture designed to reconstruct activity chains
 27 from masked inputs, leveraging the power of Transformer-based structures (26). This architecture,
 28 illustrated in Figure 4, is particularly well-suited for sequence-to-sequence tasks and incorporates
 29 several key components to enhance its effectiveness in handling temporal and contextual information
 30 inherent in human mobility patterns.

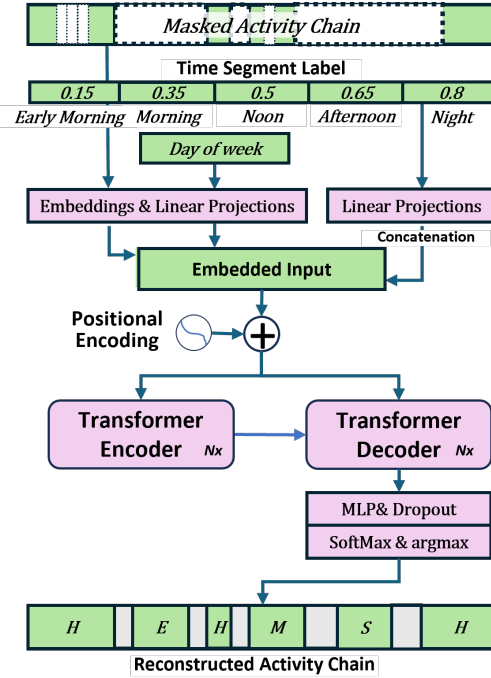


FIGURE 4: Network architecture of the mobility reconstruction model

1 **Input Preparation and Enrichment.** The model processes masked activity chains that
 2 simulate real-world data incompleteness, enhanced with temporal context through a detailed labeling
 3 scheme. Time segments are numerically valued to represent different times of day, from early
 4 morning (0.15) to night (0.8), illustrating diurnal patterns. Additionally, day-of-the-week labels
 5 capture weekly cycles, essential for analyzing human activity rhythms.

6 **Embedding and Feature Concatenation.** To optimize processing in the Transformer
 7 framework, we utilize an advanced embedding strategy. Categorical inputs, such as activity
 8 types and day-of-week indicators, are converted into dense vectors via embedding layers. These
 9 embeddings, along with time segment labels, are projected linearly to match the Transformer's
 10 dimensional requirements. The resulting vectors are then concatenated, forming an input vector that
 11 captures both temporal and contextual dimensions of the activity chain, setting a robust basis for
 12 further processing.

13 **Transformer-based Sequence Processing.** The model features three stacked Transformer
 14 blocks, each comprising an encoder and a decoder. The encoder uses self-attention to analyze
 15 embedded inputs, capturing complex dependencies across the activity chain segments beyond the
 16 limits of recurrent neural networks. The decoder then uses this processed contextual and temporal
 17 information to predict activity sequences, essential for accurately reconstructing the activity chain.

18 **Output Refinement and Activity Chain Reconstruction.** The decoder's output is refined
 19 by a multi-layer perceptron (MLP) with integrated dropout layers, which fine-tunes predictions and
 20 reduces overfitting, improving model generalization. A SoftMax layer then converts the MLP's
 21 logits into a normalized probability distribution, representing potential activity types for each time
 22 slot.

23 The culmination of this process is a fully reconstructed activity chain, with predictions for
 24 both masked and unmasked time slots. This reconstructed sequence not only serves as a direct

1 comparison to the original input chain but also demonstrates the model’s capacity to infer missing
 2 data and capture the underlying patterns of human mobility.

3 *Loss Function Design*

4 Given the encoding format of 96 time slots to describe daily activities, reconstructing the incomplete
 5 activity chain can be seen as a classification task for each time slot. The loss function tailored for
 6 the task of activity chain reconstruction. This loss function incorporates several elements to capture
 7 various aspects of the reconstruction problem, ensuring that the model learns not only to predict
 8 activities accurately but also to capture temporal dependencies and transition patterns inherent in
 9 human mobility data. The loss function comprises the following components:

10 **Cross-Entropy Loss** is commonly used to measure the dissimilarity between predicted
 11 probability distributions and true activity labels to minimize activity mismatch in each time slot.

$$12 \quad L_{CE} = - \sum_c w_c \cdot y_c \log(\hat{y}_c) \quad (3)$$

13 where y_c are the true labels for class c , and \hat{y}_c are predicted probabilities for class c . The use of
 14 class weights w_c allows for balancing the loss across potentially imbalanced activity classes.

15 **Transition Loss** focuses on accurately predicting activity transitions by comparing predicted
 16 changes in activities with the true changes using binary cross-entropy. It is designed to capture
 17 temporal dynamics by encouraging predicting changes in activities at the correct time points by
 18 penalizing incorrect transitions. This helps generate more realistic and coherent activity sequences,
 19 rather than frequently jumping between activities without any pattern.

$$20 \quad L_{TR} = - \frac{1}{N} \sum_{i=1}^N [t_i \log(\hat{t}_i) + (1 - t_i) \log(1 - \hat{t}_i)] \quad (4)$$

21 where N is the number of time steps, t_i and \hat{t}_i are true and predicted transitions at time step i (1 if
 22 activity changed, 0 otherwise).

23 **Dynamic Time Warping Loss (DTW)**, $L_{DTW} = DTW(\hat{y}, y)$, is adopted to evaluate similarity
 24 between predicted sequence \hat{y} and true sequence y using DTW distance (27).

25 Finally, the loss functions L combines three loss terms as below:

$$26 \quad L = w_1 \cdot L_{CE} + w_2 \cdot L_{TR} + w_3 \cdot L_{DTW} \quad (5)$$

27 **Semi-Supervised Iterative Transfer Learning**

28 The proposed transfer learning approach is underpinned by research indicating that over 90% of
 29 human activity patterns share similarities across different regions, captured by a limited set of
 30 human motifs (28, 29). This fundamental similarity in human behavior patterns provides a solid
 31 foundation for transferring knowledge from data-rich regions to those with limited or incomplete
 32 data. The challenge lies in effectively adapting the model to target regions while preserving the
 33 universal patterns of human behavior gleaned from the source domain.

34 As presented in Figure 3, the base model M^0 synthesizes the first dataset SD^0 , initiating an
 35 iterative cycle of model refinement. Each iteration involves the generation of a synthetic dataset SD^n
 36 from the raw incomplete activity chains, which serves to train subsequent models M^{n+1} . This cycle
 37 continues until the JSD between the synthetic and real-world data converges or meets a predefined
 38 standard, signaling the adequacy of the model to reconstruct activity chains accurately and its
 39 readiness for application in new regions.

1 *Progressive Unfreezing Approach*

2 Our fine-tuning strategy employs a progressive unfreezing approach, balancing the preservation of
 3 fundamental patterns from the source domain with adaptation to the target domain. Based on the
 4 model structure described in Figure 4, comprising embedding layers, Transformer, and MLP, we
 5 implement the following phased unfreezing:

6 In the **Initial Phase** (first quarter of epochs), only the MLP and the embedding layer are
 7 unfrozen. The MLP, being closest to the output, is responsible for the final activity classifications.
 8 Unfreezing this layer allows the model to quickly adapt its decision-making process to the new
 9 domain. Simultaneously, unfreezing the embedding layer enables fine-tuning of the basic semantic
 10 representations of activities and temporal information, such as new features, new activity definitions,
 11 and temporal patterns.

12 During the **Intermediate Phase** (second quarter of epochs), we additionally unfreeze the
 13 layer of the Transformer’s encoder and decoder closest to the input. These layers, being nearest
 14 to the input, is generally responsible for processing the most basic patterns in the sequence data.
 15 By unfreezing it last, we ensure that the fundamental knowledge learned from the source domain
 16 is preserved as much as possible while still allowing for subtle adjustments to better fit the target
 17 domain’s data characteristics.

18 In the **Final Phase** (remaining epochs), we lastly unfreeze the middle layer of the Trans-
 19 former’s encoder and decoder, which typically capture intermediate-level patterns in the data.
 20 By unfreezing it, we allow the model to adjust its representation of more complex inter-activity
 21 relationships and temporal dependencies that may be specific to the target domain.

22 This strategy is grounded in the principle that layers closer to the input learn more general,
 23 transferable features, while those closer to the output learn task-specific features (30). By keeping
 24 input-near layers of the Transformer frozen, we preserve the universal understanding of human
 25 activity patterns. The middle layers, typically most transferable (15), are unfrozen last to balance
 26 adaptation and knowledge preservation. Gradual unfreezing allows the model to capture increasingly
 27 subtle differences between domains while mitigating the risk of catastrophic forgetting. This
 28 approach aims to achieve an optimal balance between leveraging knowledge from the data-rich
 29 source domain and adapting to the specific characteristics of the target domain.

30 *Training Strategy*

31 In addition to the progressive unfreezing approach, we employ several techniques to maintain a
 32 stable learning process and enhance the model’s performance.

33 First, to avoid overfitting to the new synthetic data and ensure robustness, we retain 20% of
 34 the previous iteration’s dataset in each new training cycle. This retention strategy allows the model
 35 to continuously refine its understanding by integrating information from both new synthetic data
 36 and a portion of the previously learned data, promoting stability and preventing drastic shifts in
 37 learned patterns.

38 Additionally, real and synthetic data is differentiated during the training process. Specifically,
 39 we apply a mask-based loss weighting technique to value the contribution of real data more than

1 synthetic data in the loss computation based on the cross-entropy loss term L_{CE} , as follows:

$$\begin{aligned} L_{real} &= \frac{1}{N_r} \sum_{i=1}^N m_i \cdot L_{CE_i}, \\ L_{synthetic} &= \frac{1}{N_s} \sum_{i=1}^N (1 - m_i) \cdot L_{CE_i} \end{aligned} \quad (6)$$

3 where m_i is the mask (1 for real, 0 for synthetic), N_r and N_s are the numbers of real and synthetic
4 points. Then the total loss function becomes:

$$5 L = w_1 \cdot (w_l \cdot L_{real} + w_s \cdot L_{synthetic}) + w_2 \cdot L_{TR} + w_3 \cdot L_{DTW} \quad (7)$$

6 EXPERIMENT AND RESULTS

7 Mobility Pattern Reconstruction

8 Training Details

9 Training the base mobility pattern reconstruction model requires complete dataset, such as SCAG
10 ABM dataset and NHTS data. In this study, SCAG ABM data is selected for training the base
11 model, due to its substantial dataset size, in this study we used 700,000 samples for training,
12 200,000 samples as validation, and 100,000 samples for testing. The choice is necessitated by the
13 data-intensive nature of transformer models. In contrast, the NHTS dataset, containing only 180,000
14 samples, proves insufficient for effective training based on our preliminary experiments (9).

15 The training protocol encompassed 120 epochs with a batch size of 512. To mitigate potential
16 overfitting, we implemented regularization techniques, including dropout, L2 regularization, and
17 early stopping. Specifically, the base model training process is stratified into three distinct phases,
18 i.e., 1) Model warm-up using unmasked data for 5 epochs. 2) Training on 40% masked data for 40
19 epochs. 3) Training on 70% masked activity chain for the remaining epochs.

20 Base Model Evaluation

21 Our initial evaluation is performed on the SCAG dataset and the NHTS dataset. The model's
22 ability is tested by reconstructing 70% masked activity chains from the test set, using three types of
23 masking methods. The similarity of daily activity counts (chain length), activity duration, types,
24 and start/end times between the reconstructed and original test set activities is measured.

25 The base model M^s , trained on SCAG data, performs well when reconstructing masked
26 SCAG data, as evidenced by the close alignment of red solid (predicted) and dashed (ground truth)
27 lines in Figure 5. This performance is quantified by JSD scores between 0.001 and 0.011 (Table 2,
28 row 2). However, when applied to the NHTS dataset without modification, the model's performance
29 declines significantly, with JSD scores increasing to 0.003-0.021 (Table 2 row 3). This indicates that
30 the model trained on SCAG data (Los Angeles area) doesn't adapt well to national patterns.

TABLE 2: JSD value for similarity measurement across datasets and model performance

| JSD | Length | Duration | Type | Start Time | End Time |
|---|--------|----------|-------|------------|----------|
| SCAG vs NHTS | 0.017 | 0.009 | 0.059 | 0.018 | 0.013 |
| M^s reconstructs SCAG | 0.011 | 0.004 | 0.004 | 0.001 | 0.001 |
| M^s reconstructs NHTS | 0.021 | 0.003 | 0.017 | 0.004 | 0.007 |
| M^n reconstructs NHTS | 0.017 | 0.002 | 0.001 | 0.001 | 0.005 |

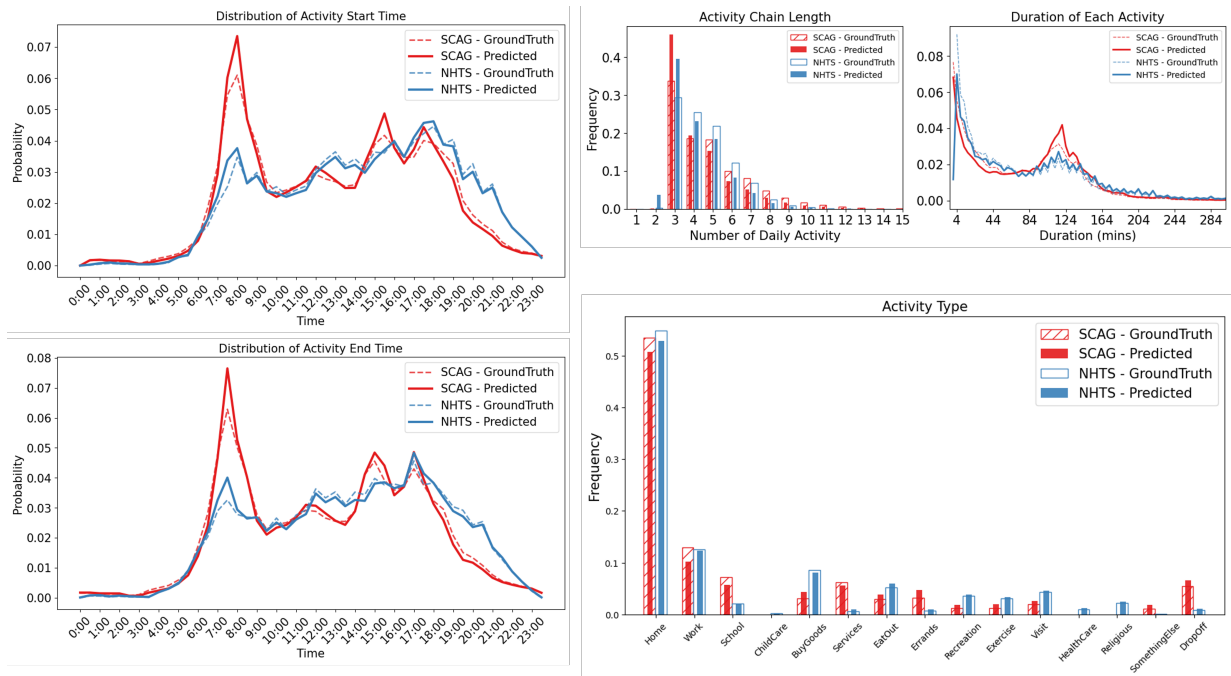


FIGURE 5: Performance evaluation on SCAG and NHTS dataset

As shown in the first row of Table 2, there are significant differences between these two datasets. The JSD scores, ranging from 0.009 to 0.059 across various activity attributes, quantify these differences. For instance, as shown in Figure 5, the activity start time distribution shows a notable peak for SCAG around 8:00 am, which is less pronounced in the NHTS data. The activity type graph reveals that SCAG data lacks representation in categories like childcare, healthcare, and religious activities, which are present in the NHTS dataset.

To address these discrepancies, we implement transfer learning for the model M^S , fine-tuning only the outer layers (embedding and MLP) of the model M^S to capture nationwide patterns from NHTS data. This approach yields marked improvements, with the NHTS dataset fine-tuned model M^N achieving JSD scores as low as 0.001 for activity types and 0.002 for durations (Table 2, row 4). Figure 5 visually confirms this improvement, showing close alignment between blue solid lines and blue dash lines lines across all distributions. These results demonstrate our algorithm's effectiveness in adapting to different geographical contexts and capturing diverse mobility patterns, despite the initial significant disparities between the SCAG and NHTS datasets.

Beyond its commendable performance in system-level JSD evaluations, the proposed model exhibits proficiency in capturing patterns of common activities, with the transfer learning successfully adapting the model from regional to national contexts. As illustrated in Figure 6, the model demonstrates remarkable accuracy in reconstructing the temporal patterns of activity start times across both datasets.

Essential activities such as home, work, and school show closely aligned patterns between the two datasets, evidenced by low JSD values (0.023, 0.021, and 0.024 respectively), highlighting the universality of these routines. Conversely, regional variations are apparent in other activities. Shopping patterns, for example, differ significantly, with SCAG data showing a midday peak (JSD 0.054) versus NHTS's more even distribution, suggesting distinct regional shopping behaviors.

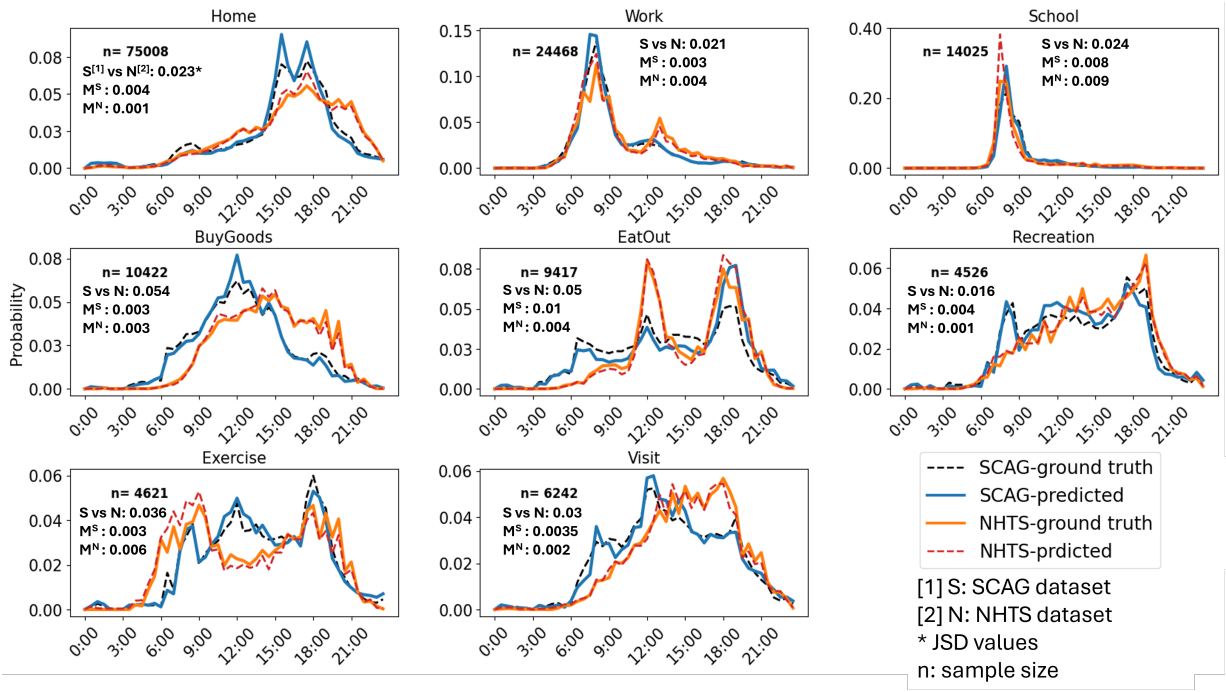


FIGURE 6: The start time of common activities reconstructed by base and its transferred model.

1 Exercise activities also vary, with NHTS indicating a preference for early morning sessions (JSD
2 0.036). These differences likely mirror varying lifestyle choices between urban Los Angeles and
3 the broader national context. The model’s consistent low M^S and M^N values, typically below 0.01,
4 confirm its efficacy in capturing these nuances, underscoring its utility for urban planning and
5 policy-making by identifying both universal and regional behavioral patterns.

6 Semi-Supervised Iterative Transfer Learning

7 The domain adaptation capability of the propose training approach is validated using a sparse GPS
8 trajectory data collected by Veraset (22) from Egypt. The trajectory data is further processed using
9 the trajectory annotation method shown in Figure 3, converting trajectories to activity chains. To
10 ensure data quality and representativeness, we implement stringent filtering criteria: only agents
11 with a minimum of 7 days of recorded activity were retained, and we exclusively utilize samples
12 that captured at least 25% of daily temporal coverage. This rigorous selection process yields a
13 substantial dataset of 479,526 samples, which we partition into training (80%) and validation (20%)
14 sets. Notably, given the absence of ground truth data in this context, A separate test set is not
15 allocated. The foundation for our transfer learning approach to the Egyptian Veraset data is the
16 model trained on NHTS dataset, selected for its comprehensive coverage of 15 distinct activity
17 types, thus providing a robust baseline for adaptation to the new geographical and cultural context,
18 i.e., from the U.S. to Egypt.

19 System-Level Analysis

20 The Semi-Supervised Transfer Learning approach demonstrates a progressive adaptation of the
21 NHTS-based model to the Egyptian context over multiple iterations, as illustrated in Figure 7 and
22 Figure 8, which visualize the the adaptation process and provide quantitative results.

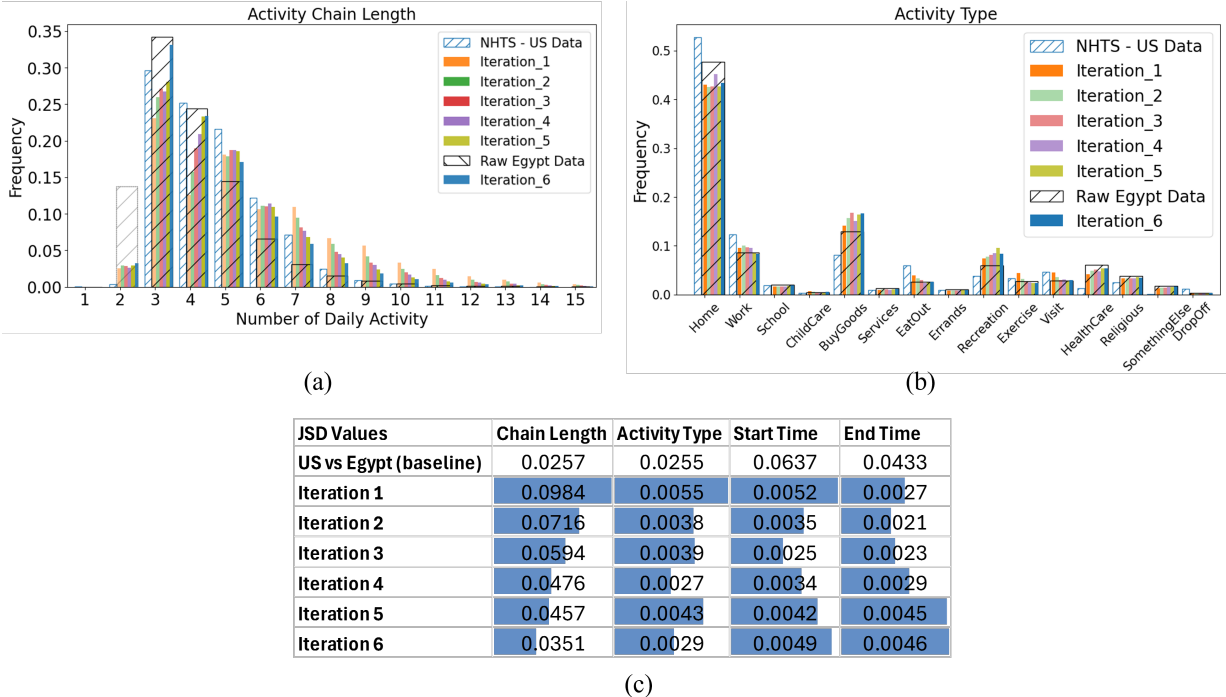


FIGURE 7: Performance evaluation: model evolution during iterative transfer learning. (a) Activity chain length, (b) type distribution, and (c) JSD value compared to raw Egypt data.

The progression of the proposed approach in adapting the NHTS-based model to the Egyptian context over multiple iterations is elaborated in Figure 7. Figure 7(a) depicts the evolution of activity chain length distribution. Notably, the raw Egyptian data's high frequency of two-activity chains (blurred bar) indicates data incompleteness rather than true behavior. As iterations progress, the model shifts from the NHTS pattern towards a more realistic Egyptian distribution, peaking at 3-4 activities per day. This demonstrates the model's ability to infer plausible patterns from incomplete data. Figure 7(b) depicts activity type frequencies. Home and Work activities remain dominant across all iterations, reflecting their universal importance. The model successfully adjusts for lower frequencies of activities like Eat out, Religious activity, and Health Care in the Egyptian context, while increasing the frequency of BuyGoods activities to match local patterns. As the iterations progress, a gradual shift is observed from the initial NHTS-US pattern towards a distribution more closely aligned with the raw Egypt data, indicating successful adaptation to local activity patterns.

The quantitative results are presented in Figure 7(c), which displays JSD values for the evaluation metrics across iterations. The first row of the table shows the dissimilarity between the U.S. (NHTS) dataset and the Egypt (Veraset) dataset, providing a baseline for comparison. Subsequent rows demonstrate the progressive adaptation through iterations. The "Length" column reveals a general decrease in JSD values from Iteration 1 (0.0984) to Iteration 6 (0.0351), indicating increasing similarity to the target distribution of activity chain lengths by %64. Activity Type JSD improves rapidly, reaching a low of 0.0027 in Iteration 4. Start Time reaches its lowest at Iteration 3 (0.0025), while End Time is lowest at Iteration 2 (0.0021), however, these two JSDs increase in later iterations.

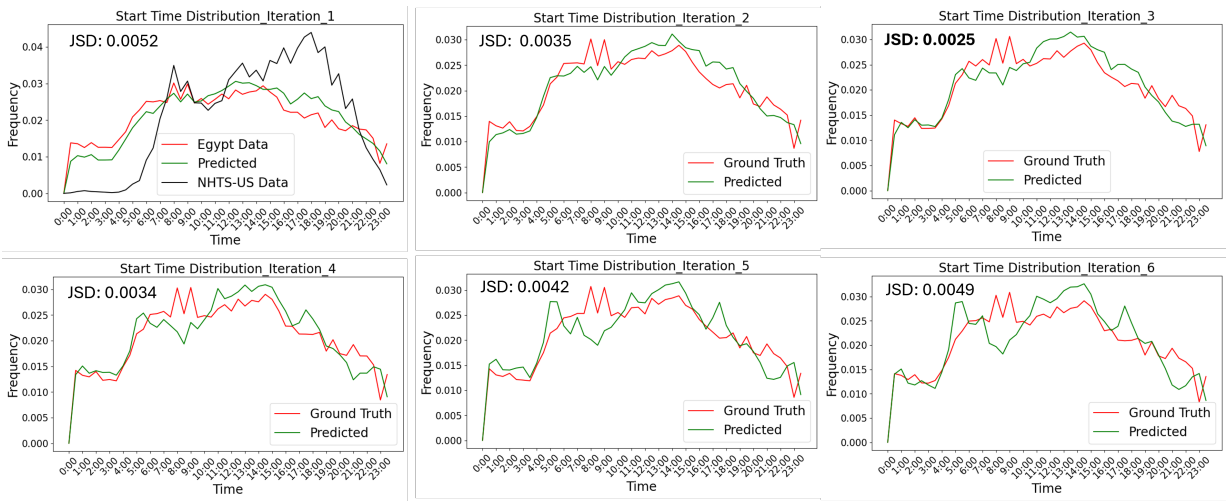


FIGURE 8: Model evolution during iterative transfer learning. Performance evaluation on start time distribution.

Building upon the previous analysis of JSD values, we further examine the temporal pattern (e.g., start time distributions) across iterations to gain deeper insights into the adaptation process. Figure 8 presents a series of graphs illustrating the start time distributions for each iteration. The initial iteration compares NHTS-US data, Egyptian data, and the model’s predictions, while subsequent iterations focus on refining predictions against Egyptian ground truth. In Iteration 1, we observe a stark contrast between the NHTS-US data, which shows a pronounced mid-day peak, and the more uniformly distributed Egyptian ground truth with multiple smaller peaks. As iterations progress, the predicted distribution increasingly aligns with the Egyptian data, reaching optimal alignment in Iteration 3 (JSD: 0.0025). This iteration effectively captures the characteristic multiple peaks of Egyptian activity patterns, particularly during morning and evening hours. However, in Iterations 4-6, a gradual divergence occurs as the model overemphasizes certain peaks while underestimating others, resulting in a slight increase in JSD values from 0.0034 to 0.0049.

Activities-Level Analysis

A detailed activity-level analysis is presented in Figure 9 and Table 3, which compare the activity start time distributions across different activity types for raw Egyptian data, NHTS US data, and two iterations of the model’s predictions. This activity-level analysis reveals the cross-cultural differences in daily activity patterns and the efficacy of the proposed iterative transfer learning approach in adapting to these differences.

TABLE 3: JSD values for start times of common activities reconstruction in Egypt

| JSD values | Home | Work | School | BuyGoods | EatOut | Exercise | HealthCare | Religious |
|------------------------|--------|--------|--------|----------|--------|----------|------------|-----------|
| US vs Egypt (baseline) | 0.0954 | 0.0886 | 0.1068 | 0.0268 | 0.0999 | 0.0581 | 0.0546 | 0.059 |
| Iteration 1 | 0.0087 | 0.0449 | 0.0262 | 0.0055 | 0.0269 | 0.0218 | 0.0115 | 0.0134 |
| Iteration 3 | 0.0094 | 0.0372 | 0.0157 | 0.0051 | 0.0197 | 0.0169 | 0.0089 | 0.0195 |

Mandatory Activities: Home activities in Egypt show a more distributed daily pattern

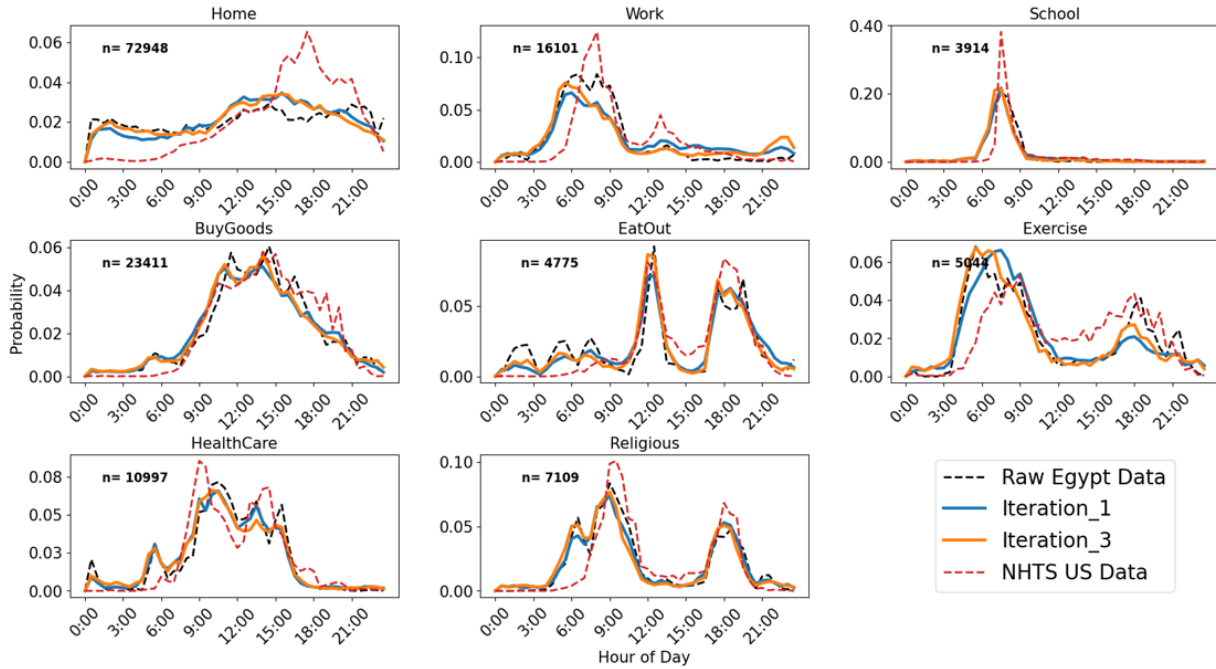


FIGURE 9: The comparison for start times of common activities in U.S., Egypt, and the model adaptation process

1 compared to the US's pronounced evening peak. As shown in Table 3, this difference is quantified by
 2 a high baseline JSD of 0.0954, which is improved to 0.0087 by Iteration 1 and at 0.0094 in Iteration
 3 3. Work activities start times exhibit a sharp morning peak in both datasets, but the Egyptian data
 4 shows a broader distribution, suggesting more varied work schedules, and the model progressively
 5 learns the pattern with JSD decreasing from 0.0886 to 0.0372 by Iteration 3. The peak time of
 6 School activity are similar across both datasets, and the model quickly capturing this similarity with
 7 JSD improving from 0.1068 to 0.0157 by Iteration 3.

8 **Non-Mandatory Activities:** BuyGoods patterns are similar between countries but with
 9 subtle timing differences, reflected in the model's quick adaptation and maintain stable through
 10 iterations (JSD: 0.0055 by Iteration 1 to 0.0051 by Iteration 3). This similarity is also presented
 11 in Eat Out activity. On the other hand, Religious activities show stronger morning and evening
 12 peaks in Egypt, likely reflecting Islamic prayer times. The model successfully adapts to these
 13 culturally specific patterns, with the JSD improving from 0.059 to 0.0134 in Iteration 1, though
 14 slightly increasing to 0.0195 in Iteration 3, still showing good overall adaptation.

15 Overall, the model effectively adapts to Egyptian activity patterns, showing rapid progress
 16 from baseline to Iteration 1 and further refinement by two more iterations. This capability is evident
 17 both visually and through decreasing JSD values, indicating a close alignment with local data
 18 while maintaining influences from the NHTS data. This analysis highlights the model's potential to
 19 generate realistic synthetic mobility data, reflecting local behaviors and cultural nuances, which is
 20 crucial for urban planning and cross-cultural behavioral studies.

1 Limitation: Synthetic Data and Model Collapse

2 Our transfer learning approach shows promise in adapting mobility patterns to the Egyptian context,
3 but it also reveals limitations in later iterations. The deterioration in model performance beyond
4 Iterations 2 and 3 aligns with recent findings by Shumailov et al.(31), who reported that "AI
5 models collapse when trained on recursively generated data". This phenomenon occurs when
6 model-generated content is indiscriminately used in training, leading to the loss of nuanced or rare
7 activities in the original data distribution.

8 The initial iterations successfully capture broad Egyptian mobility patterns. However, con-
9 tinued training on synthetic data risks amplifying minor inaccuracies and biases. This underscores
10 that synthetic data, while valuable, is not a panacea for transfer learning. Early stopping, in our case
11 at Iteration 3, appears to provide the optimal balance between local adaptation and data integrity.

12 This limitation highlights the ongoing importance of collecting data from genuine human
13 interactions. Real-world data provides essential grounding that synthetic data alone cannot replicate.
14 In conclusion, while our approach demonstrates potential in cross-cultural mobility modeling, it
15 also reveals the complexities of relying heavily on synthetic data. Balancing data augmentation
16 through transfer learning with the need for authentic, diverse data remains a critical challenge in
17 mobility modeling and AI research.

18 CONCLUSION AND FUTURE WORK

19 This study presents a novel model for reconstructing human mobility patterns by focusing on
20 semantic activity chains. Our semi-supervised approach and transfer learning techniques enable
21 the model to adapt to different regions and data availability scenarios, addressing the limitations
22 of traditional supervised learning methods. The model's effectiveness is demonstrated through
23 extensive validation with datasets from the United States and Egypt, showcasing its ability to
24 generate realistic and high-quality synthetic mobility data. These findings highlight the model's
25 potential as a powerful tool for urban planning, policy development, and transportation system
26 analysis.

27 Future work will focus on enhancing the model by incorporating socio-demographic factors
28 of agents to reconstruct more realistic activity chains for different types of people. This improvement
29 aims to provide a more personalized understanding of mobility patterns. Additionally, the current
30 model is limited to reconstructing semantic activity chains; therefore, future research will extend
31 the model to include location reconstruction. This advancement will enable a comprehensive
32 modeling of both the activities and their spatial contexts, further enriching the insights into human
33 mobility patterns. These developments will enhance the model's utility for urban planning, policy
34 development, and transportation system analysis across diverse geographical contexts and data-
35 scarce environments.

36 ACKNOWLEDGEMENTS

37 Supported by the Intelligence Advanced Research Projects Activity (IARPA) via Department of
38 Interior/Interior Business Center (DOI/IBC) contract number 140D0423C0033. The U.S. Govern-
39 ment is authorized to reproduce and distribute reprints for Governmental purposes notwithstanding
40 any copyright annotation thereon. Disclaimer: The views and conclusions contained herein are
41 those of the authors and should not be interpreted as necessarily representing the official policies or
42 endorsements, either expressed or implied, of IARPA, DOI/IBC, or the U.S. Government.

1 REFERENCES

- 2 1. Wu, H., L. Liu, Y. Yu, Z. Peng, H. Jiao, and Q. Niu, An agent-based model simulation of
3 human mobility based on mobile phone data: How commuting relates to congestion. *ISPRS
4 International Journal of Geo-Information*, Vol. 8, No. 7, 2019, p. 313.
- 5 2. Zhang, J., B. Feng, Y. Wu, P. Xu, R. Ke, and N. Dong, The effect of human mobility and
6 control measures on traffic safety during COVID-19 pandemic. *PLoS one*, Vol. 16, No. 3,
7 2021, p. e0243263.
- 8 3. Pappalardo, L., M. Vanhoof, L. Gabrielli, Z. Smoreda, D. Pedreschi, and F. Giannotti, An
9 analytical framework to nowcast well-being using mobile phone data. *International Journal
10 of Data Science and Analytics*, Vol. 2, 2016, pp. 75–92.
- 11 4. Gonzalez, M. C., C. A. Hidalgo, and A.-L. Barabasi, Understanding individual human
12 mobility patterns. *nature*, Vol. 453, No. 7196, 2008, pp. 779–782.
- 13 5. Laurila, J. K., D. Gatica-Perez, I. Aad, O. Bornet, T.-M.-T. Do, O. Dousse, J. Eberle,
14 Miettinen, et al., The mobile data challenge: Big data for mobile computing research. In
15 *Pervasive computing*, 2012.
- 16 6. Pappalardo, L., S. Rinzivillo, Z. Qu, D. Pedreschi, and F. Giannotti, Understanding the
17 patterns of car travel. *The European Physical Journal Special Topics*, Vol. 215, 2013, pp.
18 61–73.
- 19 7. Jurdak, R., K. Zhao, J. Liu, M. AbouJaoude, M. Cameron, and D. Newth, Understanding
20 human mobility from Twitter. *PloS one*, Vol. 10, No. 7, 2015, p. e0131469.
- 21 8. Liu, Y., C. Kuai, H. Ma, X. Liao, B. Y. He, and J. Ma, Semantic Trajectory Data Mining
22 with LLM-Informed POI Classification. *arXiv preprint arXiv:2405.11715*, 2024.
- 23 9. Liao, X., B. Y. He, Q. Jiang, C. Kuai, and J. Ma, Deep Activity Model: A Generative
24 Approach for Human Mobility Pattern Synthesis. *arXiv preprint arXiv:2405.17468*, 2024.
- 25 10. Chen, G., A. C. Viana, M. Fiore, and C. Sarraute, Complete trajectory reconstruction from
26 sparse mobile phone data. *EPJ Data Science*, Vol. 8, No. 1, 2019, pp. 1–24.
- 27 11. Li, M., S. Gao, F. Lu, and H. Zhang, Reconstruction of human movement trajectories from
28 large-scale low-frequency mobile phone data. *Computers, Environment and Urban Systems*,
29 Vol. 77, 2019, p. 101346.
- 30 12. Zheng, V. W., Y. Zheng, X. Xie, and Q. Yang, Collaborative location and activity recom-
31 mendations with gps history data. In *Proceedings of the 19th international conference on
32 World wide web*, 2010, pp. 1029–1038.
- 33 13. Alexander, L., S. Jiang, M. Murga, and M. C. González, Origin–destination trips by purpose
34 and time of day inferred from mobile phone data. *Transportation research part c: emerging
35 technologies*, Vol. 58, 2015, pp. 240–250.
- 36 14. Howard, J. and S. Ruder, Universal language model fine-tuning for text classification. *arXiv
37 preprint arXiv:1801.06146*, 2018.
- 38 15. Peters, M. E., S. Ruder, and N. A. Smith, To tune or not to tune? adapting pretrained
39 representations to diverse tasks. *arXiv preprint arXiv:1903.05987*, 2019.
- 40 16. Merchant, A., E. Rahimtoroghi, E. Pavlick, and I. Tenney, What happens to BERT embed-
41 dings during fine-tuning? *arXiv preprint arXiv:2004.14448*, 2020.
- 42 17. Liu, Y., M. Ott, N. Goyal, J. Du, M. Joshi, D. Chen, O. Levy, M. Lewis, L. Zettlemoyer,
43 and V. Stoyanov, Roberta: A robustly optimized bert pretraining approach. *arXiv preprint
44 arXiv:1907.11692*, 2019.

- 1 18. Luca, M., G. Barlacchi, B. Lepri, and L. Pappalardo, A survey on deep learning for human
2 mobility. *ACM Computing Surveys (CSUR)*, Vol. 55, No. 1, 2021, pp. 1–44.
- 3 19. Administration, F. H., *National Household Travel Survey*. <https://nhts.ornl.gov>,
4 2017.
- 5 20. He, B. Y., Q. Jiang, and J. Ma, Connected automated vehicle impacts in Southern California
6 part-I: Travel behavior and demand analysis. *Transportation research part D: transport and
7 environment*, Vol. 109, 2022, p. 103329.
- 8 21. Jiang, Q., B. Y. He, and J. Ma, Connected automated vehicle impacts in Southern California
9 part-II: VMT, emissions, and equity. *Transportation research part D: transport and
10 environment*, Vol. 109, 2022, p. 103381.
- 11 22. Veraset, *Global mobility and location data provider*. <https://www.veraset.com/>, 2024,
12 accessed: 2024-06-17.
- 13 23. Zheng, V. W., Y. Zheng, X. Xie, and Q. Yang, Collaborative location and activity recom-
14 mendations with GPS history data. In *Proceedings of the 19th international conference on
15 World wide web*, ACM, Raleigh North Carolina USA, 2010, pp. 1029–1038.
- 16 24. OpenStreetMap contributors, *Planet dump retrieved from https://planet.osm.org* . <https://www.openstreetmap.org>, 2017.
- 17 25. Alexander, L., S. Jiang, M. Murga, and M. C. González, Origin–destination trips by purpose
18 and time of day inferred from mobile phone data. *Transportation Research Part C*, Vol. 58,
19 2015, pp. 240–250.
- 21 26. Vaswani, A., N. Shazeer, N. Parmar, J. Uszkoreit, L. Jones, A. N. Gomez, Ł. Kaiser, and
22 I. Polosukhin, Attention is all you need. *Advances in neural information processing systems*,
23 Vol. 30, 2017.
- 24 27. Müller, M., Dynamic time warping. *Information retrieval for music and motion*, 2007, pp.
25 69–84.
- 26 28. Schneider, C. M., V. Belik, T. Couronné, Z. Smoreda, and M. C. González, Unravelling
27 daily human mobility motifs. *Journal of The Royal Society Interface*, Vol. 10, No. 84, 2013,
28 p. 20130246.
- 29 29. Cao, J., Q. Li, W. Tu, and F. Wang, Characterizing preferred motif choices and distance
30 impacts. *Plos one*, Vol. 14, No. 4, 2019, p. e0215242.
- 31 30. Yosinski, J., J. Clune, Y. Bengio, and H. Lipson, How transferable are features in deep
32 neural networks? *Advances in neural information processing systems*, Vol. 27, 2014.
- 33 31. Shumailov, I., Z. Shumaylov, Y. Zhao, N. Papernot, R. Anderson, and Y. Gal, AI models
34 collapse when trained on recursively generated data. *Nature*, Vol. 631, No. 8022, 2024, pp.
35 755–759.